Macromolecular Rapid Communications
www.mrc-journal.de

Chiral Supramolecular Polymers Assembled from Conformationally Flexible Amino-Acid-Substituted Biphenyldiimides

Grzegorz Markiewicz, Adrianna Szmulewicz, Łukasz Majchrzycki, Maarten M. J. Smulders, and Artur R. Stefankiewicz**

Hydrogen-bonded polymers are a class of highly dynamic supramolecular aggregates, whose self-assembly may be tuned by very mild external or internal stimuli. However, the rational design of chiral supramolecules remains challenging especially when flexible components are involved. The combination of the inherent weakness and dynamic nature of the intermolecular bonds that hold together such assemblies with unrestricted molecular motions introduces additional factors which may affect the self-assembly process. In this report the self-assembly of four amino acid-derived chiral biphenyldiimides into open-chain 1D supramolecular polymers is presented. While the primary driving force, COOH···HOOC hydrogen bonding, is responsible for the polymer growth in all cases, the amino acid side chains play an important role in either stabilizing or destabilizing the assemblies obtained, as deduced from studies of the thermodynamics of the self-assembly process. Furthermore, substantial differences in the structural factors governing the polymerization process between dynamic liquid and static solid are found. This work demonstrates the potential of the rather unexplored class of diimide-based organic dyes in the formation of well-organized chiral supramolecular assemblies with tunable properties.

1. Introduction

Non-covalent self-assembly is a well-established route for the spontaneous formation of supramolecular polymers with tunable complexity and functionality.[1] In contrast to covalent systems, non-covalent interactions such as hydrogen bonds show a high level of reversibility, meaning that the degree of polymerization of the supramolecular system is strongly affected by external parameters, such as concentration and temperature.[2] A large class of supramolecular polymers is based on rigid aromatic cores, which has usually a positive effect on the stability of the resulting assembly, as it not only favors π-stacking but can also pre-organize the monomers inside the assembly to enable other non-covalent bonds (e.g., hydrogen interactions).[3] To date, the self-assembly of multiply conjugated dyes has yielded numerous multifunctional materials with emerging applications in nanooptic[4] and nanoelectronic[5] devices as well as organic solar cells.[6]

Among others, perylenebisimides[7] and naphthalenediimides (NDIs)[8] are representative examples of synthons employed in the generation of supramolecular polymers. Their controlled aggregation into supramolecular polymers has enabled, for example, electronic transport,[9] tunable light emission,[10] ion channel formation[11] or probing of enzymatic reactions.[8c]

Although the importance of the primary forces governing supramolecular polymerization has become better understood over the last decades[7,8b,12] and indeed has given access to numerous non-covalent assemblies ranging from 1D polymers,[5] up to complex aggregates,[13] the rational design of chiral supramolecules consisting of flexible components remains challenging. This is mainly due to the inherent weakness of the supramolecular assemblies, where a lot of factors such as molecular conformations,[14] solute-solvent interactions,[15] guest molecules,[16] or the type of the side chains[17] may affect the self-assembly outcome.[18]

In contrast to the well-known rigid and flat diimides, biphenyldiimides (BPDIs)[19] with significant flexibility around

G. Markiewicz, A. Szmulewicz, Ł. Majchrzycki, A. R. Stefankiewicz
Center for Advanced Technology
Adam Mickiewicz University
Uniwersytetu Poznańskiego 10, Poznań 61-614, Poland
E-mail: ars@amu.edu.pl
G. Markiewicz, A. Szmulewicz, A. R. Stefankiewicz
Faculty of Chemistry
Adam Mickiewicz University
Uniwersytetu Poznańskiego 8, Poznań 61-614, Poland
M. M. J. Smulders
Laboratory of Organic Chemistry
Wageningen University
Stippeneng 4, Wageningen 6708 WE, The Netherlands
E-mail: maarten.smulders@wur.nl

The ORCID identification number(s) for the author(s) of this article can be found under https://doi.org/10.1002/marc.202200767

DOI: 10.1002/marc.202200767

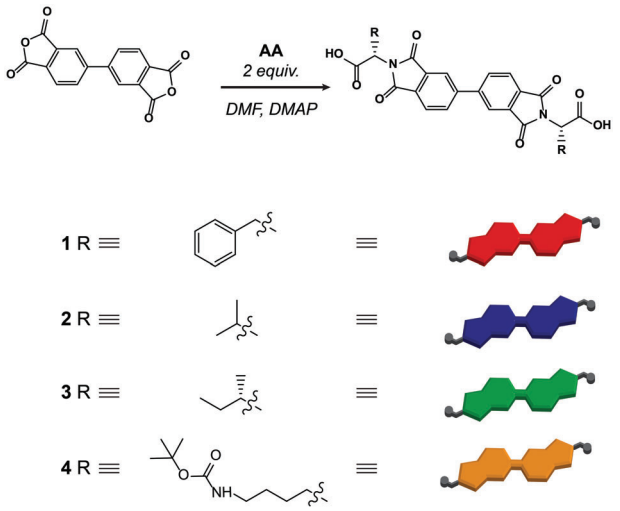

Figure 1. Synthesis of the enantiomerically pure biphenyldiimides **1**, **2**, **3**, **4** from 3,3′,4,4′-biphenyltetracarboxylic dianhydride (BPDA) and the appropriate amino acid (AA).

the single bond of the central aromatic core are much less explored but recently attracted attention as the versatile building blocks for the generation of nanooptic,[20] nanoelectronic,[21] and photocatalytic[22] materials. While those intramolecular motions might be restricted either by the introduction of bulky substituents,[23] or cyclization,[20,21,24] to the best of our knowledge, the unrestricted BPDIs have not yet been successfully employed in the formation of chiral supramolecular polymers.

Following our previous experience, with the synthesis[19] and self-assembly of amino acid-derived diimides,[16,25] we decided to utilize BPDIs decorated with homochiral α-amino acids of different functionality for the formation of supramolecular polymers both in solution and solid state. Namely, aliphatic, aromatic and hydrogen bonding-competitive amino acid residues were planted on 3,3',4,4'-positions via diimide bridges, leaving 2,2',5,5'-positions in the proximity of the singular bond unoccupied (**Figure 1**).

In this report we describe the self-assembly of four amino acid-derived BPDIs into chiral 1D chain-type supramolecular polymers. While the assemblies obtained were found to be held together by COOH···HOOC hydrogen bonds in all cases, the amino acid side chains played an important role in stabilizing or destabilizing the polymeric structures with surprisingly opposite effects in solution and solid state. That is, we found the aromatic side chains of phenylalanine to increase the stability of polymers in the solution. However, this effect is not related to the formation of π–π interactions, but rather to the bulkiness of the side chains, and it subsequently hampered the aggregation in the solid state. In contrary, the introduction of additional hydrogen bonding moieties in the amino acid side chains disrupted the self-assembly in solution, by the preferential formation of competitive intramolecular interactions. The latter, however, when shifted to the solid state, contributed to the formation of larger supramolecular aggregates. Ultimately, the thermodynamic parameters of the self-assembly process in solution were revealed, and the polymerization was determined to proceed via an isodesmic mechanism unless competitive interactions occur.

2. Results and Discussion

The enantiomerically pure components **1**–**4** were obtained according to the procedure previously reported by us.[19] The microwave-assisted condensation between L-amino acid and 3,3′,4,4′-biphenyltetracarboxylic dianhydride (BPDA) under basic conditions yielded each of the four corresponding homochiral diimide monomers equipped with carboxylic acid units introduced for the formation of hydrogen-bonded assemblies (Figure 1). Four different L-amino acid side chains were employed, in order to investigate the influence of the side chain on the self-assembly outcome and thermodynamic stability of the structures obtained. Namely, while the phenylalanine side chain in **1** could potentially introduce steric and shielding effects as well as the supplementary π-stacking interactions, the valine (**2**) and isoleucine (**3**) side chains will not show such features, although in **3** additional chiral centers are present. Ultimately, monomer **4**, apart from being highly flexible, possesses additional competitive hydrogen bonding sites within the side chain that may stabilize or destabilize the self-assembly outcome.

The components **1**–**4** were expected to aggregate via hydrogen bonding interactions between COOH units, and/or π-stacking forces between aromatic moieties (between the biphenyl cores and aromatic side chains in the case of **1**). Additionally, the formation of weak CH···O=C interactions involving imide units as observed, for example, in the case of naphthalene diimide was also taken into account.[26]

Non-covalent assemblies in solution are known to undergo continuous reversible dissociation-association processes upon changes in concentration or temperature, both directly affecting the degree of aggregation.[12] In order to confirm that the presented BPDIs indeed self-assemble in non-competitive solvents, variable temperature (VT) ^{1}H NMR experiments were performed for **1**. The solution of **1** (1.0×10^{-3} M) in 1,1,2,2-tetrachloroethane (TCE-d_2) was first heated up to 338 K, and then gradually cooled down to 228 K, at a rate of −1 K min^{-1}. It is worth to mention, that the α-CH groups are in the closest proximity to the COOH sites, so one can expect their resonance to be strongly affected by the hydrogen bonding-driven polymerization. Furthermore, the aromatic resonances originating from the BPDI core and/or phenylalanine side chains should be affected in the case of the formation of π–π interactions as well as the possible atropoisomeric rotation within the biphenyl core. Upon cooling, the gradual broadening of all the resonances was observed with the most indicative signal being the α-CH group from the amino acid side chain (**Figure 2**a; Figure S5, Supporting Information). At 338 K this resonance was recorded as a well resolved *dd* (J = 10.6, 6.0 Hz) at 5.27 p.p.m., which gradually shifted into a broad singlet at 5.12 p.p.m. at 228 K. However, apart from strong broadening the aromatic resonances of both biphenyl core and phenylalanine side chains of **1** (Figure S5, Supporting Information), these signals were found to be essentially unaffected by the increase in the aggregation degree (≤0.05 p.p.m. upfield shifts), suggesting that π–π stacking interactions do not play any significant role in the supramolecular polymerization of **1**. Given the strong broadening, one can also conclude the atropoisomeric rotation is rather dynamic (on the NMR time scale), so the self-assembly retains – at least partial – flexibility of the biphenyl core. Those results are also consistent with the variable temperature UV spectra of **1**

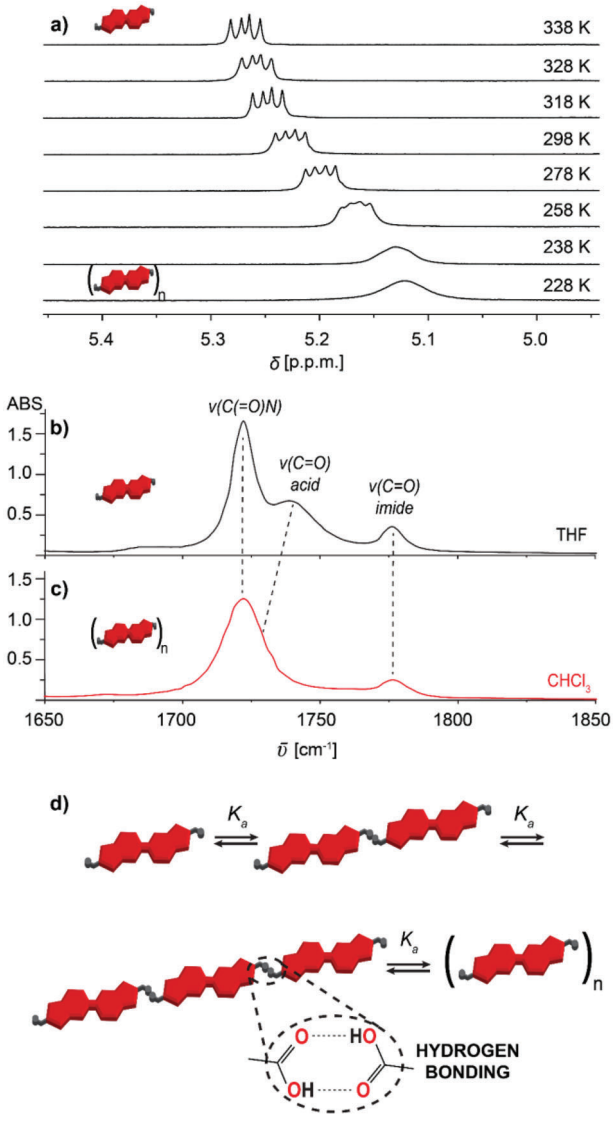

Figure 2. Self-assembly of **1** as followed by variable temperature (VT) ^{1}H NMR and FT-IR analysis. a) VT ^{1}H NMR (600 MHz, TCE-d_2) spectra of α-CH resonance of **1** (1.0×10^{-3} M) (For full spectra see Figure S5, Supporting Information). b) Part of the FT-IR spectrum of **1** (C=O stretch) as recorded in THF (1.0×10^{-2} M) with assigned bands (For full spectrum see Figure S7, Supporting Information). c) Part of the FT-IR spectrum of **1** (C=O stretch) as recorded in $CHCl_3$ (1.0×10^{-2} M) (For full spectrum see Figure S7, Supporting Information). d) Schematic representation of the proposed mechanism of the self-assembly of **1**.

in $CHCl_3$ where no indicative bathochromic shifts (that could be ascribed to the formation of π–π interactions involving biphenyl chromophores) were observed upon the increase of the degree of aggregation (Figure S6, Supporting Information).

In order to directly observe the hydrogen bonding sites and subsequently the supramolecular interactions themselves, the self-assembly of polymers based on components **1**–**4** was additionally followed by infrared spectroscopy (FT-IR) in tetrahydrofuran (THF) (Figure 2b) and $CHCl_3$ (Figure 2c) solutions (See Supporting Information for details). THF was used as a highly polar and competitive solvent, in which solvent-solute interactions are favored over hydrogen-bonded self-assembly. On the other hand, $CHCl_3$ as a non-competitive solvent of low polarity promotes solute-solute interactions, and therefore induces the hydrogen bonding-driven polymerization of **1**–**4**. As shown in Figure 2b,c, the $\nu(C{=}O)^{acid}$ band of the COOH moieties of **1** shift from 1739 (b) to 1723 cm^{-1} (c) when dissolved THF and $CHCl_3$, respectively. The latter is accompanied by the reduced intensity of the $\nu(O{-}H)^{free}$ band (Figure S7, Supporting Information). The observed shift of −17 cm^{-1} in $\nu(C{=}O)^{acid}$ stretch frequency is consistent with the dimerization of the aliphatic acids via COOH···HOOC hydrogen bonding,[27] which in the case of terminal diacids (**1**-**4**) is responsible for the generation of the polymer chain between the components (Figure 2d).

In contrast, both $\nu(C{=}O)^{imide}$ (1777 cm^{-1}), as well as $\nu(C(=O)N)^{imide}$ (1723 cm^{-1}) bands, were found to be completely unaffected by the solvent change. Given that the formation of any kind of hydrogen bonds by imido groups should substantially affect their IR stretching frequencies, as recently shown by us for NDI assemblies,[25b] one can conclude that the imido groups from the BPDI are not involved in the polymerization process in this case. Essentially identical FT-IR responses were observed also for **2**, **3**, and **4**, with ≈−17 cm^{-1} shifts in $\nu(C{=}O)^{acid}$ stretch frequencies in all cases (Figures S8–S10, Supporting Information), with one additional observation concerning the *tert*-butyloxycarbonyl (Boc) groups in the side chains of **4**. Namely, Boc groups also have shown signs of hydrogen bonding interactions when dissolved in $CHCl_3$ by the strong broadening of $\nu(N{-}H)^{amide}$ band ≈3300 cm^{-1} (vide infra). Taking into account the FT-IR and NMR data, one can conclude that the self-assembly of **1**–**4** is driven solely by COOH···HOOC interactions, and that neither π-stacking nor any kind of hydrogen bonding involving imide units plays any significant role in the aggregation process.

Based on our previous experience with chiral hydrogen-bonded assemblies,[17a,25b,25c] we decided to also follow the self-assembly of **1**–**4** by variable temperature Circular Dichroism (VT-CD). VT-CD spectra of **1**–**4** recorded in $CHCl_3$ revealed that their self-assembly is manifested by the appearance of a negative Cotton band at ≈320 nm, the intensity of which strongly depended on the temperature of the solution: the CD intensity increased with decreasing temperature, suggesting that upon cooling the chiral monomers assemble into a chiral (i.e., CD active) polymer. In order to study the thermodynamics of the self-assembly, the solutions of components **1**–**4** in $CHCl_3$ (1.0×10^{-3} M) were heated up to 330 K, and then slowly cooled down to 250 K (cooling rate −1 K min^{-1}), while monitoring the changes in CD intensity (Figures S11,S12, Supporting Information). The cooling rate of −1 K min^{-1} was found to be slow enough to achieve thermodynamic control over the polymerization process, as well as to observe the assembly-disassembly equilibria in a reasonable experimental time (Figure S13, Supporting Information). As a reference, all four components were also dissolved in a competitive solvent, that is, THF (1.0×10^{-3} M), and their CD spectra were recorded at 298 K in order to determine any residual chiral effects at the monomeric state. Indeed, due to the close proximity of the chiral centers and biphenyl chromophore, the diimides showed minor CD activity also at the monomeric level (Figure S14, Supporting Information), which is most pronounced for component **1** (vide infra).

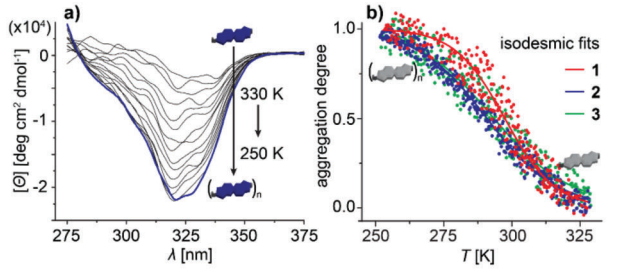

c)	1_n	2_n	3_n
ΔH_m [kJ mol^{-1}]	−88.0 ±4.6	−60.7 ±1.5	−56.2 ±3.1
T_m [K]	298 ±0.4	291 ±0.6	293 ±1.0
K_a [10^3 M^{-1}] at 273 K	11.7	2.9	2.9
DP_N at 273 K	4.02	2.26	2.28

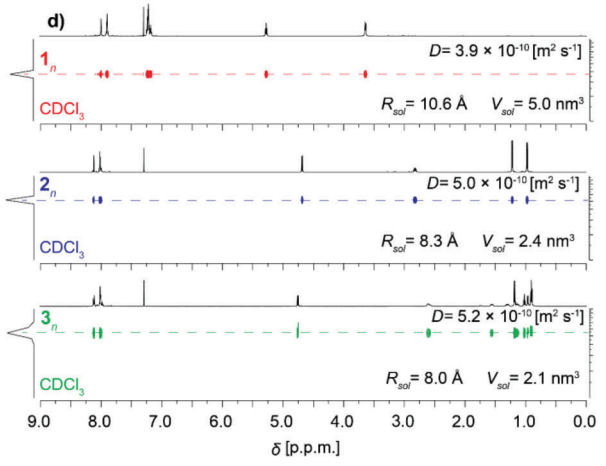

Figure 3. Self-assembly of **1**–**3** as followed by variable temperature Circular Dichroism (VT-CD) and diffusion-orderded NMR spectroscopy (DOSY). a) VT-CD spectra recorded during cooling of solution of **2** in $CHCl_3$ (1.0×10^{-3} M, cooling rate −1 K min^{-1}). b) Normalized VT-CD signal changes (at 318 nm) recorded during cooling of solutions of **1**–**3** in $CHCl_3$ (1.0×10^{-3} M, cooling rate −1 K min^{-1}) with isodesmic fits (solid lines). c) Thermodynamic parameters calculated from fitting of the data to the isodesmic model. d) DOSY NMR (600 MHz, $CDCl_3$) spectra recorded for $\mathbf{1}_n$ (red), $\mathbf{2}_n$ (blue) and $\mathbf{3}_n$ (green) (1.0×10^{-2} M, $T = 298$ K). Inset: solvodynamic radii and volumes calculated according to the Stokes-Einstein equation.

Upon cooling of the $CHCl_3$ solutions of **1**–**4**, the gradual increase in the intensity of the negative Cotton band at ≈320 nm was observed (**Figure 3**a for **2**, for **1**, **3**, and **4** see in Figure S11, Supporting Information). Plotting those changes as a function of temperature revealed that the self-assembly of three components (**1**, **2**, and **3**) proceeds via an S-shaped transition from monomer (at high temperature) to aggregate (at low temperature), indicative of a non-cooperative isodesmic supramolecular polymerization model[28] (Figure 3b). In contrast, **4** revealed a rather sharp transition, which will be discussed separately.

The subsequent fitting of the (normalized) VT data to an isodesmic model confirmed that the self-assembly of **1**, **2**, and **3** follow the isodesmic pathway and is indeed enthalpy-driven as indicated by the negative enthalpy change ΔH_m in all cases (Figure 3c). The enthalpy-driven isodesmic polymerization is in line with the previous studies about the COOH···HOOC hydrogen-bonded assemblies.[17a]

The isodesmic polymerization mechanism of **1**, **2**, and **3** was further supported by the concentration-dependent ^{1}H NMR analysis (Figure S15, Supporting Information). However, the limited solubility of compounds in $CDCl_3$ (determined $C_{sat} = 3.0$–7.0×10^{-2} M at $T = 298$ K) hampered the registration of the full aggregation curves in those experiments, hence the results of the fittings are less precise than the ones obtained in VT-CD experiments.

From a thermodynamic point of view, $\mathbf{1}_n$ was found to be the most stable with $\Delta H_m = -88.0$ kJ mol^{-1} and $T_m = 298$ K. The stability of $\mathbf{2}_n$ and $\mathbf{3}_n$ polymers was found to be significantly lower than that of $\mathbf{1}_n$, but nearly identical between $\mathbf{2}_n$ and $\mathbf{3}_n$ with $\Delta H_m = -60.7$ or -56.2 kJ mol^{-1} and $T_m = 291$ or 293 K for $\mathbf{2}_n$ and $\mathbf{3}_n$, respectively. The results confirmed that the two additional chiral centers introduced by the isoleucine side chains in **3** (in comparison to valine chains in **2**) have a negligible effect on the thermodynamics of their aggregation. In fact, the thermodynamic parameter describing the self-assembly of $\mathbf{2}_n$ and $\mathbf{3}_n$ polymers are identical (with the differences being in the range of standard deviations of the fittings), and the only effect observed for the secondary chiral centers is the reduced molar ellipticity of the $\mathbf{3}_n$ assembly (Figure S11, Supporting Information).

While the similarity of $\mathbf{2}_n$ and $\mathbf{3}_n$ could be expected, it was somehow surprising to find the difference of ≈−30 kJ mol^{-1} in the ΔH_m of $\mathbf{1}_n$ without any experimental evidence that intermolecular π-stacking interactions play a role in its self-assembly. Also, the phenylalanine side chains and biphenyl core are too far away from each other for significant intramolecular π-stacking to occur (Figure S16, Supporting Information). The increased stability of $\mathbf{1}_n$ seems to be related to both the presence of bulky substituents and to solvent mask effects. The former one being responsible for the restriction of the molecular motions at the monomeric level (thus orienting the carboxylic binding sites prior to the self-assembly) and the latter one for the isolation of the binding sites from solvation by the bulky phenyl rings from the phenylalanine side chains, as observed in other system studied by us.[29] In fact, CD spectra revealed that **1** is the only component that possesses a significant residual Cotton effect at the monomeric state (both at elevated temperatures in $CHCl_3$ and when dissolved in THF, See Figures S11 and S14, Supporting Information) with the same sign as of $\mathbf{1}_n$ but of lower intensity. This might be associated to the reduction of the conformational lability at the monomeric level, which seems to have a highly positive effect on the overall thermodynamic stability of $\mathbf{1}_n$ in comparison to $\mathbf{2}_n$ and $\mathbf{3}_n$.

The isodesmic polymerization observed for **1**, **2** and **3** typically results in rather short (degree of polymerization $DP_N < 10$) assemblies.[12] In line with this, diffusion-ordered NMR spectroscopy (DOSY) in $CDCl_3$ (1.0×10^{-2} M, $T = 298$ K) revealed small solvodynamic radii of 10.6, 8.3, and 8.2 Å for **1**, **2**, and **3** respectively (Figure 3d).

In contrast to the self-assembly of **1**–**3**, the polymer formed by the *N*(Boc)lysine derived **4** was found to be very unstable above 298 K (**Figure 4**a). Namely, upon cooling of its $CHCl_3$ solution

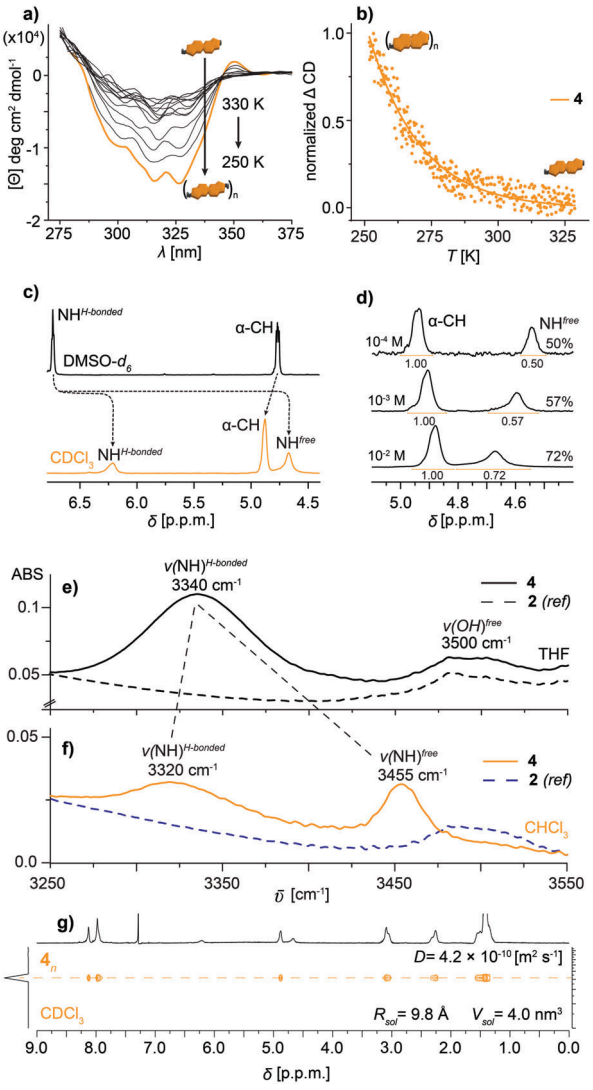

Figure 4. Self-assembly of **4** as followed by variable temperature Circular Dichroism (VT-CD), ^{1}H NMR, FT-IR, and diffusion-ordered NMR spectroscopy (DOSY). a) VT-CD spectra recorded during cooling of solution of **4** in $CHCl_3$ (1.0×10^{-3} M, cooling rate −1 K min^{-1}). b) Normalized VT-CD signal changes (at 318 nm) recorded during cooling of solution of **4** in $CHCl_3$ (1.0×10^{-3} M, cooling rate −1 K min^{-1}). c) Comparison between ^{1}H NMR (600 MHz) spectra of **4** (NH resonances) recorded in DMSO-d_6 and $CDCl_3$ (1.0×10^{-2} M, $T = 298$ K). d) Concentration-dependent ^{1}H NMR (600 MHz, $CDCl_3$) spectra of **4** recorded at $T = 298$ K. e) Part of the FT-IR spectrum of **4** (N-H stretch) as recorded in THF (1.0×10^{-2} M) with assigned bands (For full spectrum see Figure S10, Supporting Information). f) Part of the FT-IR spectrum of **1** (N-H stretch) as recorded in $CHCl_3$ (1.0×10^{-2} M) (For full spectrum see Figure S10, Supporting Information). g) DOSY NMR (600 MHz, $CDCl_3$) spectrum recorded for $\mathbf{4}_n$ (1.0×10^{-2} M, $T = 298$ K). Inset: solvodynamic radii and volumes calculated according to the Stokes-Einstein equation.

(1.0×10^{-3} M), **4** showed a nearly zero CD signal down to 290 K, below which a sharp increase in the CD intensity was observed, indicative of the polymerization process taking place (Figure 4b). This polymerization could not be successfully described by the isodesmic polymerization model, and the sharp change suggests that the self-assembly of **4** is not a simple enthalpy-driven process (as in the case of **1**–**3**) but it rather competes with the secondary processes, for example, intramolecular binding like in ring-chain polymerization reactions.[12] However, in contrary to the intermolecular supramolecular polymerization, intramolecular interactions should be concentration independent, with both processes being sensitive toward the temperature. Indeed, concentration-dependent ^{1}H NMR analysis of **4** in $CDCl_3$ revealed a linear correlation between δ α-CH resonance and log(C) (Figure S17, Supporting Information), the result being inconsistent neither with the sigmoidal dependence of the isodesmic polymerization nor with the sharp transition observed for **4** upon cooling on the CD spectra (Figure 4b).

In order to explain the polymerization of **4**, we decided to look deeper into its molecular structure and hydrogen bonding sites. Molecular modeling revealed that the protected lysine side chains in **4** possess sufficient flexibility to fold and form intramolecular COOH···NHOC hydrogen bonding between COOH centers and Boc protecting group and thus occupy both hydrogen bonding acceptor and donor sites in the COOH group (Figure S18, Supporting Information), mimicking the COOH···HOOC interactions observed for polymers.

Interestingly, at high concentrations ($\geq 1.0 \times 10^{-2}$ M) in $CDCl_3$ the NH groups of **4** were observed by ^{1}H NMR as two broad resonances, that is, at 4.7 p.p.m. assigned to the unbounded amides (NH^{free}), and at 6.2 p.p.m. assigned to the H-bonded groups ($NH^{H\text{-}bonded}$) (Figure 4c). This apparent equilibrium was found to be dynamic at 298 K, as evidenced by the exchange peaks between NH^{free}:$NH^{H\text{-}bonded}$ resonances recorded on the ROESY NMR spectrum (Figure S19, Supporting Information). Noteworthy, when dissolved in a highly competitive solvent (dimethyl sulfoxide, DMSO-d_6) the NH groups of **4** appeared as a single, well-resolved triplet ($J = 5.6$ Hz) at 6.7 p.p.m. due to solvation (NH···O=S) (Figure 4c).

Although the $NH^{H\text{-}bonded}$ resonance at 6.2 p.p.m. in $CDCl_3$ disappears upon dilution ($\leq 1.0 \times 10^{-3}$ M) due to a very strong line broadening, ^{1}H NMR analysis revealed that the relative ratio between NH^{free} and $NH^{H\text{-}bonded}$ groups is concentration-dependent (when integrated against the non-exchangeable α-CH signal), with NH^{free} favored at high concentrations (72% at 1.0×10^{-2} M), and disfavored upon dilution (50% at 1.0×10^{-4} M) (Figure 4d). Similar conclusion might be put forward based on the analysis of ν(N—H) bands observed for **4** on FT-IR spectra.[27] Namely, in THF a single ν(N—H) band was observed at 3350 cm^{-1}, corresponding to the solvated ($NH^{\cdots O^{THF}}$) groups (Figure 4e). Upon solvent change into $CHCl_3$, this stretching splits into two separated bands: $\nu(N\text{—}H)^{H\text{-}bonded}$ at 3320 and $\nu(N\text{—}H)^{free}$ at 3490 cm^{-1} (Figure 4f), which is consistent with the equilibrium between NH^{free}:$NH^{H\text{-}bonded}$ observed on the ^{1}H NMR spectra. Unfortunately, the effect of the hydrogen bonding could not be observed for the amido C=O stretching bands, as those fully overlap with the broad stretching of the imido groups from the biphenyldiimide central core at 1725 cm^{-1} (Figure S10, Supporting Information).

Taking into account that from the monomers of **1**–**4**, only **4** possess these competitive intramolecular hydrogen bonding sites in the side chain, it is clear that the polymerization of **1**–**3** can proceed from the molecularly dissolved state with free COOH centers, to COOH···HOOC hydrogen-bonded polymers (n X ⇄ X_n). However, this is not the case for component **4**, where the

competitive interactions occur, and the polymerization energy must overcome not only the entropic costs of the self-assembly, but also the energy of the (energetically similar) intramolecular forces ($n\ \mathbf{4}^{H\text{-}bonded} \rightleftarrows n\ \mathbf{4}^{free} \rightleftarrows \mathbf{4}_n$). Therefore, polymerization of **4** in solution appears to not follow neither isodesmic mechanism, nor a ring-chain mechanism, since the binding sites for intramolecular and intermolecular processes are not equal.[12] Despite the competitive polymerization pathway, the process is dynamic and fully reversible at ±1 K min^{-1}, even at high concentrations (1.0×10^{-2} M) as confirmed by the reversible VT ^{1}H NMR analysis, without any notable hysteresis between cooling and heating cycles (Figures S20 and S21, Supporting Information).

The competition between intra- and intermolecular equilibria is operative even at the conditions favoring assembly (1.0×10^{-2} M, $T = 233$ K) (Figures S20 and S21, Supporting Information). Subsequently, the system does not saturate with $\mathbf{4}_n$, that is, the apparent aggregation degree in the $CDCl_3$ solution does not reach 100% at any experimentally available conditions, in line with the observed transition in the above-discussed variable temperature CD experiment. Those competitive equilibria however yield (1.0×10^{-2} M, T= 298 K) the assemblies with solvodynamic radius of 9.9 Å (Figure 4g) similar to the isodesmic polymers of **1**, **2**, **3**.

Ultimately, the self-assembly of **1**–**4** was also studied in the solid state by Atomic Force Microscopy (AFM). Each component was dissolved in $CHCl_3$ (5.0×10^{-4} M), and then drops (10 µL) of those solutions were spin-coated onto freshly cleaved mica surfaces. Due to the good wettability of mica by $CHCl_3$ as well as its high volatility, the deposition assisted by spin-coating led to the uniform deposition of the assemblies in a form of aggregates with a typical surface area in tens of nm^2 (**Figure 5**a-d).

Elongated structures with aspect ratios in the range between 2 and 6 and thickness in the range of 10–50 nm were obtained. The average length of the aggregates was found to be 60 ± 26 nm, 180 ± 120 nm, 100 ± 52 nm, and 130 ± 74 nm for assemblies of $\mathbf{1}_n$, $\mathbf{2}_n$, $\mathbf{3}_n$, and $\mathbf{4}_n$, respectively. However, the distribution of aggregate length was very wide and cannot be treated as a structural indicator. It is clearly seen from the AFM images, that the aggregates of each of the molecules exhibit their own, specific apparent height. The typical value of the aggregate's median apparent height equals 0.6, 1.1, 1.3, and 1.55 nm respectively for the $\mathbf{1}_n$, $\mathbf{2}_n$, $\mathbf{3}_n$, and $\mathbf{4}_n$ (Figure 5e). Surprisingly, major discrepancies between the apparent assembly size in the solid and thermodynamic stability of the assemblies of **1**–**4** in the solution were observed. Namely while in the diluted solutions the self-assembly of $\mathbf{4}_n$ was found to be weak, due to competitive intramolecular interactions, the secondary binding sites seem to play important role in the solid-state aggregation on the surface, which results in an increase in the assembly apparent height most likely related to the cross-linking of the individual polymeric chains. On the other hand, the bulky phenyl substituents in **1**, which stabilize the $\mathbf{1}_n$ polymer in solution, substantially restrict its aggregation on the solid matrix, leading to the reduction of their apparent height due to the repulsive forces between polymer chains. The presented results are an interesting example of a supramolecular system, where different factors govern the processes of the self-assembly of small polymeric structures under dynamic solution conditions, and their full aggregation in the closely packed and static solid. In fact, similar discrepancies were also observed

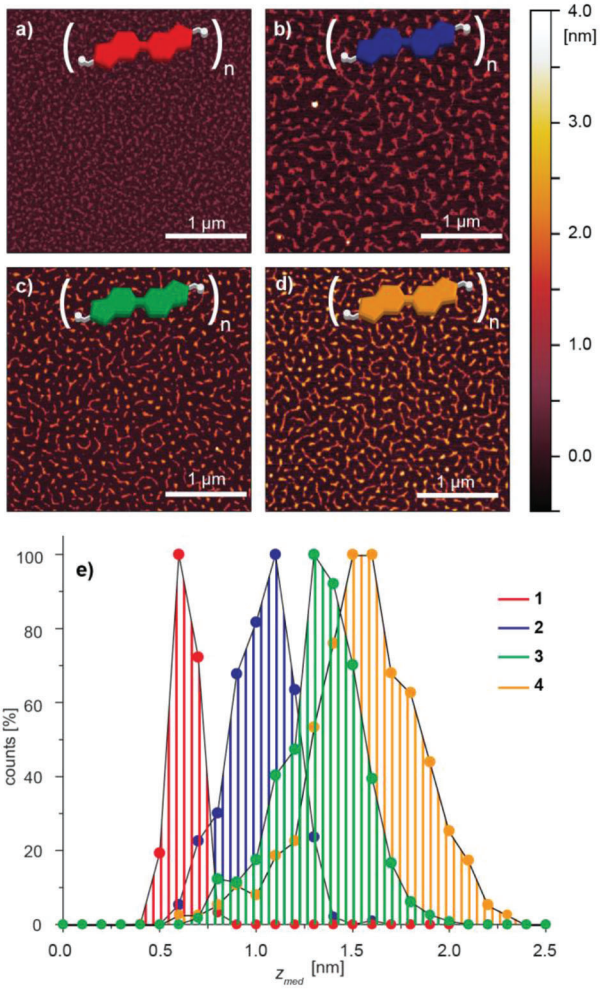

Figure 5. Solid state characterization of the $\mathbf{1}_n$, $\mathbf{2}_n$, $\mathbf{3}_n$, and $\mathbf{4}_n$ assemblies by Atomic Force Microscopy (AFM) as obtained by spin-coating the solutions in $CHCl_3$ (5.0×10^{-4} M) onto mica surfaces. a) AFM image of $\mathbf{1}_n$; b) AFM image of $\mathbf{2}_n$; c) AFM image of $\mathbf{3}_n$; d) AFM image of $\mathbf{4}_n$; e) AFM median apparent height of the $\mathbf{1}_n$, $\mathbf{2}_n$, $\mathbf{3}_n$, $\mathbf{4}_n$ assemblies.

in recent years for the benzene-1,3,5-tricarboxamide derivatives, where depending on the conditions, the self-assembly may yield dimeric structures, columnar polymers, or their mixtures in solutions and solid crystals.[17b,17c,30]

3. Conclusion

The self-assembly of four chiral biphenyl diimides was studied in solution and in the solid state. The result shows that those compounds in solution spontaneously form non-covalent chain-type supramolecular polymers, as a result of formation of COOH···HOOC hydrogen bonding bridges. While the aggregates obtained are of similar topology, significant differences in their stability were observed, as a result of the influence of the amino acid side chains. Namely, while the aromatic side chains were shown to increase the overall stability of the assembly, by restricting the molecular motions and shielding the COOH···HOOC bridges, the presence of secondary hydrogen

bonding sites destabilizes the assembly and disturbs the polymerization process due to preferential formation of intramolecular interactions in diluted solutions. However, in the solid state, the above features seem to have a positive role and an increase in the size of the aggregates is observed. We believe, the use of conformationally labile building blocks based on biphenyl cores opens up new pathways for the formation of chiral supramolecular polymers, which we aim to explore in the future.

Supporting Information

Supporting Information is available from the Wiley Online Library or from the author.

Acknowledgements

This work was financially supported by National Science Centre (Grant PRELUDIUM UMO-2017/25/N/ST5/00451). GM is supported by the Foundation for Polish Science (FNP) START program.

Conflict of Interest

The authors declare no conflict of interest.

Data Availability Statement

The data that support the findings of this study are available from the corresponding author upon reasonable request.

Keywords

amino-acids, biphenyldiimides, hydrogen-bonding, self-assembly, supramolecular polymerization

Received: September 26, 2022
Revised: November 9, 2022
Published online:

[1] a) X. W. Zhan, A. Facchetti, S. Barlow, T. J. Marks, M. A. Ratner, M. R. Wasielewski, S. R. Marder, *Adv. Mater.* **2011**, *23*, 268; b) R. Dong, Y. Zhou, X. Huang, X. Zhu, Y. Lu, J. Shen, *Adv. Mater.* **2015**, *27*, 498.
[2] A. Sorrenti, J. Leira-Iglesias, A. J. Markvoort, T. F. A. de Greef, T. M. Hermans, *Chem. Soc. Rev.* **2017**, *46*, 5476.
[3] F. Xu, S. Crespi, L. Pfeifer, M. C. A. Stuart, B. L. Feringa, *CCS Chem.* **2022**, *4*, 2212.
[4] T. Schembri, J. H. Kim, A. Liess, V. Stepanenko, M. Stolte, F. Würthner, *Adv. Opt. Mater.* **2021**, *9*, 2100213.
[5] A. P. H. J. Schenning, E. W. Meijer, *Chem. Commun.* **2005**, 3245.
[6] B. Mahlmeister, R. Renner, O. Anhalt, M. Stolte, F. Würthner, *J. Mater. Chem. C* **2022**, *10*, 2581.
[7] F. Würthner, C. R. Saha-Möller, B. Fimmel, S. Ogi, P. Leowanawat, D. Schmidt, *Chem. Rev.* **2016**, *116*, 962.
[8] a) M. A. Kobaisi, S. V. Bhosale, K. Latham, A. M. Raynor, S. V. Bhosale, *Chem. Rev.* **2016**, *116*, 11685; b) S.-L. Suraru, F. Würthner, *Angew. Chem., Int. Ed.* **2014**, *53*, 7428; c) M. Kumar, P. Brocorens, C. Tonnelé, D. Beljonne, M. Surin, S. J. George, *Nat. Commun.* **2014**, *5*, 5793.
[9] C. E. Finlayson, R. H. Friend, M. B. J. Otten, E. Schwartz, J. J. L. M. Cornelissen, R. J. M. Nolte, A. E. Rowan, P. Samorì, V. Palermo, A. Liscio, K. Peneva, K. Müllen, S. Trapani, D. Beljonne, *Adv. Funct. Mater.* **2008**, *18*, 3947.
[10] a) Z. Chen, V. Stepanenko, V. Dehm, P. Prins, L. D. A. Siebbeles, J. Seibt, P. Marquetand, V. Engel, F. Würthner, *Chem. - Eur. J.* **2007**, *13*, 436; b) M. R. Molla, D. Gehrig, L. Roy, V. Kamm, A. Paul, F. Laquai, S. Ghosh, *Chem. - Eur. J.* **2014**, *20*, 760; c) Y. Wang, Y. Jiang, X. Zhu, M. Liu, *J. Phys. Chem. Lett.* **2019**, *10*, 5861.
[11] P. Talukdar, G. Bollot, J. Mareda, N. Sakai, S. Matile, *J. Am. Chem. Soc.* **2005**, *127*, 6528.
[12] T. F. A. de Greef, M. M. J. Smulders, M. Wolffs, A. P. H. J. Schenning, R. P. Sijbesma, E. W. Meijer, *Chem. Rev.* **2009**, *109*, 5687.
[13] a) P. A. Korevaar, T. F. A. de Greef, E. W. Meijer, *Chem. Mater.* **2014**, *26*, 576; b) P. A. Korevaar, S. J. George, A. J. Markvoort, M. M. J. Smulders, P. A. J. Hilbers, A. P. H. J. Schenning, T. F. A. de Greef, E. W. Meijer, *Nature* **2012**, *481*, 492; c) D. Gorl, X. Zhang, V. Stepanenko, F. Würthner, *Nat. Commun.* **2015**, *6*, 7009.
[14] J.-F. Xu, Z. Huang, L. Chen, B. Qin, Q. Song, Z. Wang, X. Zhang, *ACS Macro Lett.* **2015**, *4*, 1410.
[15] R. E. Kieltyka, A. C. H. Pape, L. Albertazzi, Y. Nakano, M. M. C. Bastings, I. K. Voets, P. Y. W. Dankers, E. W. Meijer, *J. Am. Chem. Soc.* **2013**, *135*, 11159.
[16] A. R. Stefankiewicz, E. Tamanini, G. D. Pantoş, J. K. M. Sanders, *Angew. Chem., Int. Ed.* **2011**, *50*, 5724.
[17] a) N. Ponnuswamy, G. D. Pantoş, M. M. J. Smulders, J. K. M. Sanders, *J. Am. Chem. Soc.* **2012**, *134*, 566; b) A. D. Lynes, C. S. Hawes, E. N. Ward, B. Haffner, M. E. Möbius, K. Byrne, W. Schmitt, R. Pal, T. Gunnlaugsson, *CrystEngComm* **2017**, *19*, 1427; c) A. Desmarchelier, B. G. Alvarenga, X. Caumes, L. Dubreucq, C. Troufflard, M. Tessier, N. Vanthuyne, J. Idé, T. Maistriaux, D. Beljonne, P. Brocorens, R. Lazzaroni, M. Raynal, L. Bouteiller, *Soft Matter* **2016**, *12*, 7824.
[18] T. Schnitzer, M. D. Preuss, J. van Basten, S. M. C. Schoenmakers, A. J. H. Spiering, G. Vantomme, E. W. Meijer, *Angew. Chem., Int. Ed.* **2022**, *61*, e202206738.
[19] M. Konopka, G. Markiewicz, A. R. Stefankiewicz, *RSC Adv.* **2018**, *8*, 29840.
[20] Z. Wang, R. Song, Y. Zhang, T. Zhang, X. Zhu, J. Zeng, W. Zhang, Z. Zhao, N. Yan, G. He, *ChemPhotoChem* **2020**, *4*, 59.
[21] Z. Wang, B. Zhang, Y. Zhang, N. Yan, G. He, *RSC Adv.* **2020**, *10*, 31049.
[22] Y. Kofuji, S. Ohkita, Y. Shiraishi, H. Sakamoto, S. Tanaka, S. Ichikawa, T. Hirai, *ACS Catal.* **2016**, *6*, 7021.
[23] a) N. Kawano, M. Okigawa, N. Hasaka, I. Kouno, Y. Kawahara, Y. Fujita, *J. Org. Chem.* **1981**, *46*, 389; b) F. Leroux, *ChemBioChem* **2004**, *5*, 644.
[24] Z. Wang, X. Zhu, S. Zhang, L. Xu, Z. Zhao, G. He, *Adv. Opt. Mater.* **2021**, *9*, 2001764.
[25] a) M. A. Squillaci, G. Markiewicz, A. Walczak, A. Ciesielski, A. R. Stefankiewicz, P. Samorì, *Chem. Commun.* **2017**, *53*, 9713; b) G. Markiewicz, M. M. J. Smulders, A. R. Stefankiewicz, *Adv. Sci.* **2019**, *6*, 1900577; c) N. Ponnuswamy, A. R. Stefankiewicz, J. K. M. Sanders, G. D. Pantoş, *Top. Curr. Chem.* **2012**, *322*, 217.
[26] G. D. Pantoş, P. Pengo, J. K. Sanders, *Angew. Chem., Int. Ed.* **2007**, *46*, 194.
[27] a) B. H. Stuart, *Infrared spectroscopy: fundamentals and applications*, Wiley, Hoboken, NJ **2004**; b) S. Ogi, V. Stepanenko, J. Thein, F. Würthner, *J. Am. Chem. Soc.* **2016**, *138*, 670.
[28] M. M. J. Smulders, M. M. L. Nieuwenhuizen, T. F. A. de Greef, P. van der Schoot, A. P. H. J. Schenning, E. W. Meijer, *Chem. - Eur. J.* **2010**, *16*, 362.
[29] G. Markiewicz, A. Jenczak, M. Kołodziejski, J. J. Holstein, J. K. M. Sanders, A. R. Stefankiewicz, *Nat. Commun.* **2017**, *8*, 15109.
[30] a) A. Frank, A. Bernet, K. Kreger, H.-W. Schmidt, *Soft Matter* **2020**, *16*, 4564; b) F. Perlitius, A. Walczak, M. Čonková, G. Markiewicz, J. Harrowfield, A. R. Stefankiewicz, *J. Mol. Liq.* **2022**, *367*, 120511.

